Received: 8 September 2023 | Revised: 15 December 2023 | Accepted: 2 January 2024

DOI: 10.1111/php.13908

RESEARCH ARTICLE

Photophobotaxis in the filamentous cyanobacterium *Phormidium lacuna*: Mechanisms and implications for photosynthesis-based light direction sensing

Elina Schwabenland | Caroline Janine Jelen | Nora Weber | Tilman Lamparter

Karlsruhe Institute of Technology, JKIP, Karlsruhe, Germany

Correspondence
Tilman Lamparter, Karlsruhe Institute of Technology, JKIP, Fritz Haber Weg 4, D-76137 Karlsruhe, Germany.
Email: tilman.lamparter@kit.edu

Abstract

Cyanobacterium *Phormidium lacuna* filaments move from dark to illuminated areas by twitching motility. Time-lapse recordings demonstrated that this photophobotaxis response was based on random movements with movement reversion at the light–dark border. The filaments in the illuminated area form a biofilm attached to the surface. The wild-type and the *pixJ* and *cphA* mutants were investigated for photophobotaxis at diverse wavelengths and intensities. CphA is a cyanobacterial phytochrome; PixJ is a biliprotein with a methyl-accepting chemotaxis domain and is regarded as a phototaxis photoreceptor in other species. The *cphA* mutant exhibited reduced biofilm surface binding. The *pixJ* mutant was characterized as a negative photophobotaxis regulator and not as a light direction sensor. 3-(3,4-dichlorophenyl)1,1-dimethylurea (DCMU) blocks electron transfer in PS II. At concentrations of 100 and 1000 μM DCMU, photophobotaxis was inhibited to a greater extent than motility, suggesting that PSII has a role in photophobotaxis. We argue that the intracellular concentrations of regular photoreceptors, including CphA or PixJ, are too small for a filament to sense rapid light intensity changes in very weak light. Three arguments, specific inhibition by DCMU, broad spectral sensitivity, and sensitivity against weak light, support photosynthesis pigments for use as photophobotaxis sensors.

KEYWORDS

chemotaxis, MCP, Oscillatoria, phytochrome, PixJ, type IV pili

INTRODUCTION

Cyanobacteria are prokaryotic organisms that perform oxygenic water-splitting photosynthesis, which is the most efficient way to convert sunlight energy into energy for biomolecule synthesis. Light-driven electron transfer from water through photosystems I and II (PS I and PS II) results in NADP reduction and proton gradient formation, which in turn drives ATP synthesis.[1,2] Cyanobacteria and photosynthetic eukaryotes share the same oxygenic evolution mechanism and kind of photosystems. To maximize light capture and minimize damage caused by excessively strong

[Correction added on 01 February, 2024 after first online publication: Author name Carolina Janine Jelen is corrected to Caroline Janine Jelen in this version.]

light, sessile photosynthetic organisms adapt their growth speed or direction to light conditions, whereas motile photosynthetic organisms move toward the light if the light is weak or away from the light if the light is strong and deleterious.[3,4] Two principal modes of movement toward light can be distinguished: phototaxis and photophobotaxis. During phototaxis, directional movement is driven by the direction of light, that is, light comes from the side, and the organisms move to this side or away from it. During photophobotaxis, light comes from above or below, and cells move toward or away from the illuminated area perpendicular to the light direction. In cyanobacteria, phototaxis has been described in single-celled species,[5] whereas photophobotaxis has been described in filamentous Oscillatoriales.[6] Both the cyanobacterial phototactic and photophobotactic movements are mediated by type IV pili,[7,8] a transmembrane multiprotein complex that generates a moving force by expelling and retracting PilA protein threads.

Both directional light responses require one or more photoreceptors for light perception. Additionally, a mechanism that forms a signal gradient of activated photoreceptors within the cell, filaments, or over time is required. For single-celled *Synechocystis* sp. PCC6803[9] and *Synechococus* elongatus UTR[10] phototaxis, it has been demonstrated that unilateral light was focused within the cell onto the light-avoiding side by light refraction during the transition into the optically dense cell interior. An uneven light distribution within the cell leads to an uneven, gradual photoreceptor stimulation, given that the photoreceptor does not fluctuate. This can lead to a polar distribution of type IV pili on one side of the cell which can mechanistically elucidate how unilateral light induces directional motion.[11] In photophobotaxis of filamentous cyanobacteria, light direction is probably sensed by a dark avoidance reaction,[8] but details are yet not clear.

The photoreceptor responsible for light direction sensing in cyanobacteria remains obscure. Several chromoprotein knockout mutants exhibit changes in phototaxis. If a single photoreceptor is responsible for light direction sensing, knockout of the respective gene would result in non-phototactic movement. However, such a clear response was generally not found. In the single-celled cyanobacterium, *Synechocystis* sp. PCC 6803, wherein most experiments on phototaxis have been performed, knockouts of PixJ,[12] Cph2,[13] PixD/E,[14,15] and UirS[16] typically result in changes in phototaxis from positive to negative, or under special conditions, in phototaxis weakening. Only in *pixJ*-knockout *Synechococcus elongatus* UTEX 3055, phototaxis was lost under certain conditions. A switch from positive to negative phototaxis cannot be regarded as a phototaxis loss but rather as an increase in sensitivity. PixD is a BLUF protein,[7] and PixJ, Cph2, and UirS are cyanobacteriochromes with one or more bilin-binding GAF proteins. PixJ proteins contain an additional methyl-accepting chemotactic sensor domain. In bacterial chemotaxis, this domain is responsible for adaptation of the substrate receptors sensitivity by methylation and demethylation.[17] Any photoreceptor for which an effect on phototaxis is observed could act through signal transduction cascade modulation. Additionally, it has been suggested that photosynthesis could play a role in cyanobacterial phototaxis.[18,19] In photophobotaxis of the filamentous cyanobacterium *Phormidium uncinatum*, the light reaction was inhibited by DCMU, which blocks the photosynthetic electron transfer at PS II.[18] However, in phototaxis of *Synechocystis sp* PCC 6803, no DCMU effect or a weak effect was observed.[5,20]

We studied photophobotaxis of the filamentous cyanobacterium *Phormidium lacuna* HE10DO. This strain was isolated from a marine rock pool in the North Sea island Helgoland.[21] Like other cyanobacteria, *P. lacuna* moves in the direction of their longitudinal axis by twitching on surfaces. Filaments of Oscillatoriales also undergo a second type of motion that takes place in liquid medium, where filaments oscillate against each other in transverse direction with respect to their longitudinal axis.[8] Through natural transformation, several genes encoding type IV pili components have been knocked out in *P. lacuna*. In all mutants, twitching motility along the agar surface and lateral/transverse movement in the liquid medium were inhibited, indicating that both types of movement were mediated by type IV pili.

When we irradiated *P. lacuna* filaments on agar with light from the side to induce phototaxis, we found no directional movement toward the light.[8] However, light from below induced photophobotaxis, that is, the filaments collected within the light spot. This response was accompanied by the attachment of the filaments to the Petri dish surface at the position of the light spot. In all type IV pili gene mutants, photophobotaxis was drastically reduced or lost, as expected.[8] In a cyanobacterial phytochrome *cphA* mutant, photophobotaxis and surface attachment were reduced.[8]

In this study, we performed extended photophobotaxis studies on the wild type, the *cphA* knockout, and a newly generated *pixJ* knockout of *P. lacuna*. We verified that CphA modulates surface attachment and biofilm formation. PixJ has been found to act as a negative photophobotaxis regulator, and photosynthesis inhibitor studies have suggested that PS II could be involved in photophobotaxis.

MATERIALS AND METHODS

Strains and mutants

The *P. lacuna* HE10DO strain was used for all experiments. The genome of this strain has been sequenced.[21]

The filaments were cultivated in f/2$^+$ seawater medium[21,22] in 20- or 50-mL culture flasks under continuous 200 µmol m^{-2}s^{-1} white LED light under agitation at 25°C. The generation of *cphA* mutant has been described previously.[8] The gene was interrupted at position 1103 of the 2532 bp open reading frame.

The *pixJ* mutant was generated by homologous insertion of a kanamycin (Kn) cassette into the coding region, 60 bp downstream of the start codon. To this end, a 1067 bp sequence was amplified by PCR using the primers pixJ_fwd and pixJ_rev (primers in Table S1) and cloned into the pGEMT vector (Promega). Primers SS_KpnI_pixJ_fwd and pixJ_SS_PacI_rev were utilized for a PCR reaction to linearize the new vector. The Kn resistance cassette was amplified using the primers SS_PacI_KanR_fwd and KanR_SS_KpnI_rev. Both PCR products were digested with PacI and KpnI and ligated with each other. The final circular product contained approximately 500 bp upstream and downstream of position 60 of the *pixJ* coding sequence, interrupted by a Kn cassette.

Phormidium lacuna transformation was performed as previously described[8,23,24] with slight modifications. *P. lacuna* was cultivated in f/2 medium until $A_{750\,nm} = 0.35$. The cell culture was concentrated 20-fold via centrifugation. Ten microgram vector DNA were mixed with 100 µL cell suspension and pipetted in the center of an f/2 agar plate (1.5% Bacto agar and 75 µg/mL Kn). This procedure was repeated eight times (800 µL cells). After 2 weeks, the filaments were transferred to agar plates with 500 µg/mL Kn and kept for another 2 weeks on this medium. Thereafter, single growing filaments were isolated and cultivated on fresh agar plates with 500 µg/mL Kn. After ca 1 week, propagation was continued in liquid medium with 100 µg/mL Kn. To test for integration into the homologous site and the completeness of segregation, we performed PCR using inner and outer primer pairs (Table S1). The inner primer pair binds at the 5′ and 3′ ends of the integrated sequence, and the outer primer pair binds only 5′ and 3′ outside the integrated sequence. For cultivation, mutants were always grown in medium with 100 µg/mL Kn, for experiments the cells were transferred into medium without antibiotics. Complete segregation into all chromosomes was tested by PCR,[8] see Figure S1 as example for several tests. A gel with PCR of the *pixJ* insertion mutant and outer primers demonstrating homologous insertion and complete segregation at the expected position is depicted in Figure S1.

Phototaxis and photophobotaxis

cphA and *pixJ* cultures were maintained in f/2$^+$ medium[8] containing 250 µg/mL Kn. For phototaxis and photophobotaxis experiments, strains were cultivated in *medium* without Kn for 10–20 days on a shaker at 25°C in plastic flasks in white light (100 µmol m^{-2}s^{-1}) until $OD_{750\,nm}$ was 0.3 or higher. Before phototaxis or photophobotaxis, the cultures were treated with UltraThurrax (*Silentcrusher M von Heidolph*) for 3 min at 10,000 rpm. The $OD_{750\,nm}$ was measured and adjusted to 0.25 (for most experiments) or 0.2 (for inhibition experiments). The OD was measured using a *Uvikon XS photometer* (Goebel Instrumentelle Analytik, Au, Germany).

For photophobotaxis irradiation, 8 mL *P. lacuna* Ultraturrax-treated filaments were brought into a 5 cm Petri dish, which was placed on a plastic holder from a 3D printer with a 5-mm LED (Figure 1C,D).[8,24] The LEDs were fixed at the end of a 15-mm-long vertical tunnel. Each LED was mounted to shine upward toward the center of the Petri

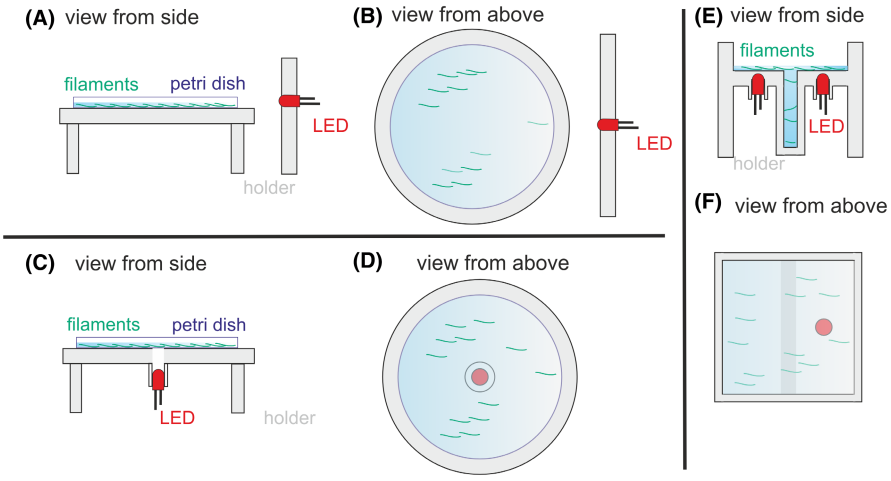

FIGURE 1 Experimental arrangements for phototaxis and photophobotaxis. A and B arrangement for unilateral irradiation, C and D arrangement for photophobotaxis, light from below, E and F design for ditch experiment. On either side of the ditch there is one LED, in f one LED is drawn, the other is dark.

dish (see Figure 1C,D). For phototaxis, the same holder was placed vertically so that the Petri dish was irradiated from the side (Figure 1A,B). Light intensities were measured using a Skye photometer SKP 215 (Skye Instruments Ltd., Wales). The intensities of far-red and weak light were determined by measuring the resistance of the photoresistor PDV-P5003 (Luna Optielectronics), which was calibrated by comparison with a Skye photometer. The irradiation time in steady-state photophobotaxis experiments was usually 2 days.

In photophobotaxis experiments, a biofilm formed within the irradiated area. The Petri dish was photographed using a smartphone camera without moving the dish away from its original position. The Petri dish was gently shaken manually for 3 s and photographed again. The diameters and areas of the circles were measured using the ImageJ software (NCBI). The comparison before and after shaking is a measure for the stability of the biofilm. For the 3-(3,4-dichlorophenyl)1,1-dimethylu rea (DCMU) and methylviologen (MV) inhibition experiments, self-programmed Python 3.9 algorithm was utilized to determine biofilm areas. The algorithm detects the number of pixels in the biofilm central area. To this end, each image was converted into a black and white image to distinguish the pixels in the biofilm area from the background. All images were first cropped to a small square area in the middle to remove unwanted light reflections. The number of black pixels (i.e., biofilm) were integrated, and the mm^2 area was computed using the entire Petri dish area as a reference. The filaments that gathered outside the central circle were often above the threshold. These pixels were manually excluded. Wild-type samples from both evaluation modes had slightly different mean values, and the values of the second evaluation were normalized accordingly. Other data evaluation and statistical analyses were performed with the OriginPro 2023 software. For the significance of differences, we always chose the Mann–Whitney test (MW) for different mean values[25] of the program OriginPro 2023 (www.originlab.com). An error probability of <0.05 was considered as significant.

Infrared time lapse recording

For time lapse studies on motility, 8 mL of a Ultrasound-treated filament suspension ($OD_{750\ nm} = 0.1$) were poured into a 5 cm Petri dish. The Petri dish was placed on a holder containing a 650 nm LED adjusted to 5 $\mu mol\, m^{-2} s^{-1}$, which was placed in the center of the Petri dish and which illuminated the sample from below. This light was also used for camera recordings in that region. The region around the red light was illuminated with infrared light from six 850 nm LEDs from below through an opaque glass for even illumination. Images were captured every 2 s, and videos were made at 25 images per second. A conventional microscope with a Bresser (Rhede, Germany Deep Sky) telescope camera was used. The TOUPview (www.toupview.com) software was used for inspection, and movies were built using Kdenlive (http://kdenlive.org).

Mobility assays

For motility assays that were performed after the inhibitor treatments, ca. 100 µL filaments were transferred to a new Petri dish containing agar medium (1% Bacto agar with f/2 medium). Images of filaments were taken at 1 min intervals through 10× objective as above for ca. 30 min. Two subsequent images in false red or false green color were combined using ImageJ software (NCBI). The moving distance was determined by the extension of red or green at the end of a filament. For each treatment, the average of ca. 50 cells was taken.

Inhibitor treatment

The herbicide 3-(3,4-dichlorophenyl)1,1-dimethylurea (DCMU) was used to block the electron transfer in PS II. This compound binds to PS II at the plastoquinone B (PQ_B) binding site.[26] DCMU stock solutions were prepared in ethanol at 100 mM and 100 µM concentrations. From here, $f/2^+$ solutions were prepared with final concentrations of 0.01–1000 µM DCMU. Ethanol controls were prepared with 1% ethanol, the highest concentration in the DCMU series.

Methyl viologen (paraquat, MV) is a PS I electron transfer quencher.[27] Stock solutions were prepared in $f/2^+$ medium and the solutions containing 0.01–1000 µM MV were prepared by dilution.

RESULTS

The *P. lacuna* genome contains one phytochrome gene, one PixJ gene, and 28 other cyanobacteriochrome genes

We investigated photophobotaxis using two different knockout mutants, *cphA* and *pixJ*. Phytochromes are involved in many plant and bacterial light responses. CphA is the only cyanobacterial phytochrome identified in *P. lacuna*, and the *cphA* mutant showed a moderate phenotype in earlier photophobotaxis analyses.[8] Phytochromes have a characteristic PAS-GAF-PHY domain arrangement and the majority of phytochromes have a C-terminal histidine kinase (Figure 2C). In bacteria, genes within an

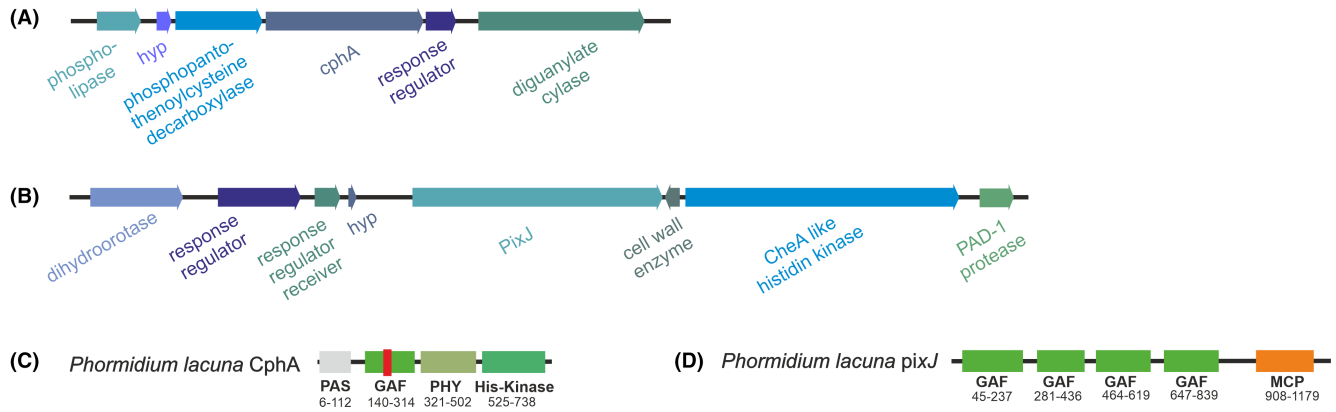

FIGURE 2 CphA and PixJ of *Phormidium lacuna*. (A) Gene arrangement around *cphA*. From left to right: phospholipase, hypothetical protein, *cphA*, response regulator, diguanylate cyclase. (B) Gene arrangement around *pixJ*, from left to right: dihydroorotase, response regulator, response regulator receiver, hypothetical protein, *pixJ*, CheA-like histidine kinase, PAD-1 protease. (C) Domain arrangement of CphA with PAS, GAF PHY domains and the C-terminal histidine kinase. The red bar indicates the chromophore binding cysteine. (D) Domain arrangement of PixJ. The red bars indicate the chromophore binding cysteines.

operon and their neighboring genes share common functions. The gene 5′ of *cphA* encodes for a phosphopantothenoylcysteine decarboxylase, which is a part of coenzyme A biosynthesis. The gene further 5′ encodes a hypothetical protein (Figure 2A). The gene 3′ of *cphA* encodes a response regulator. Response regulators are signaling proteins phosphorylated by histidine kinases. The co-arrangement of phytochromes and response regulators genes is often observed in bacterial systems.[28] Further 3′ there is a gene encoding a protein with a diguanylate cyclase (GGDEF) and a phosphodiesterase (EAL) domain. Both domains act antagonistically in the synthesis or degradation of cyclic di-GMP, a second messenger for biofilm formation.[29] The genes are separated by a 300-bp promoter sequence.

PixJ belongs to a group of cyanobacteriochromes that comprise one or more bilin-binding GAF domain(s) combined with other domains of diverse types. PixJ proteins have a methyl acceptor chemotaxis domain (MCP) at their C-termini and an N-terminal HAMP domain at the MCP. In other cyanobacteria, PixJ is regarded as photoreceptor for phototaxis.[7,10,30,31] Like *T. elongatus* PixJ,[31] *P. lacuna* PixJ has four GAF domains; GAF domains 2, 3, and 4 have a chromophore-binding cysteine at a position homologous to other cyanobacteriochromes or phytochromes, whereas GAF domain 1 has no cysteine at this position. The domain arrangement of PixJ is depicted in Figure 2D.

The genes 5′ of *pixJ* encode dihydroorotase, an enzyme in the pyrimidine metabolism, a response regulator, a response regulator receiver, a hypothetical protein, and a chemotaxis sensor histidine kinase (Figure 2B). The genes 3′ of *pixJ* encode an enzyme of the cell wall biosynthesis, a CheA like histidine kinase, and a protease.

In addition to *cphA* and *pixJ*, the *P. lacuna* genome contains 28 other genes that encode proteins with GAF domains. Each of these proteins can have more than one GAF domain, the number of 4 is however only reached by *pixJ*. The overall number of GAF domains was 52, of which 20 contained chromophore-binding Cys. We constructed a phylogenetic tree, wherein all *P. lacuna* GAF domains and the PFAM seed[32] had additional 438 GAF domains from cyanobacteria, other bacteria, and eukaryotes (Figures S1,S2). In this tree, GAF 2, 3, and 4 of PixJ clustered closely together with other cyanobacterial GAF domains of cyanobacteriochromes, whereas N-terminal GAF 1 of PixJ belonged to another cluster that appeared next to the cluster above. As expected, CphA GAF domain clustered with GAF domains of other phytochromes. Cyanobacterial GAF domains with chromophore-binding Cys are located close to the phytochromes, which strengthens the hypothesis that cyanobacterial GAF domains originate from phytochromes.[33]

Unilateral light induced a weak phototactic response in wild type and *cphA* and a strong response in *pixJ*

We previously observed that filaments on agar medium that were irradiated with light from the side did not move toward or away from the light.[8] Here, we found that filaments in Petri dishes with liquid medium (without agar) and irradiated from the side (Figure 1A,B) showed a directional response. Some wild-type and *cphA* filaments migrated toward the light, and a weak accumulation of filaments was observed along the light beam (Figure 3A–C). The *pixJ* mutant exhibited a significantly (Mann–Whitney test, MV) stronger response, in line with the higher *pixJ* sensitivity observed in other experiments described below. These results show that *P. lacuna* can undergoes

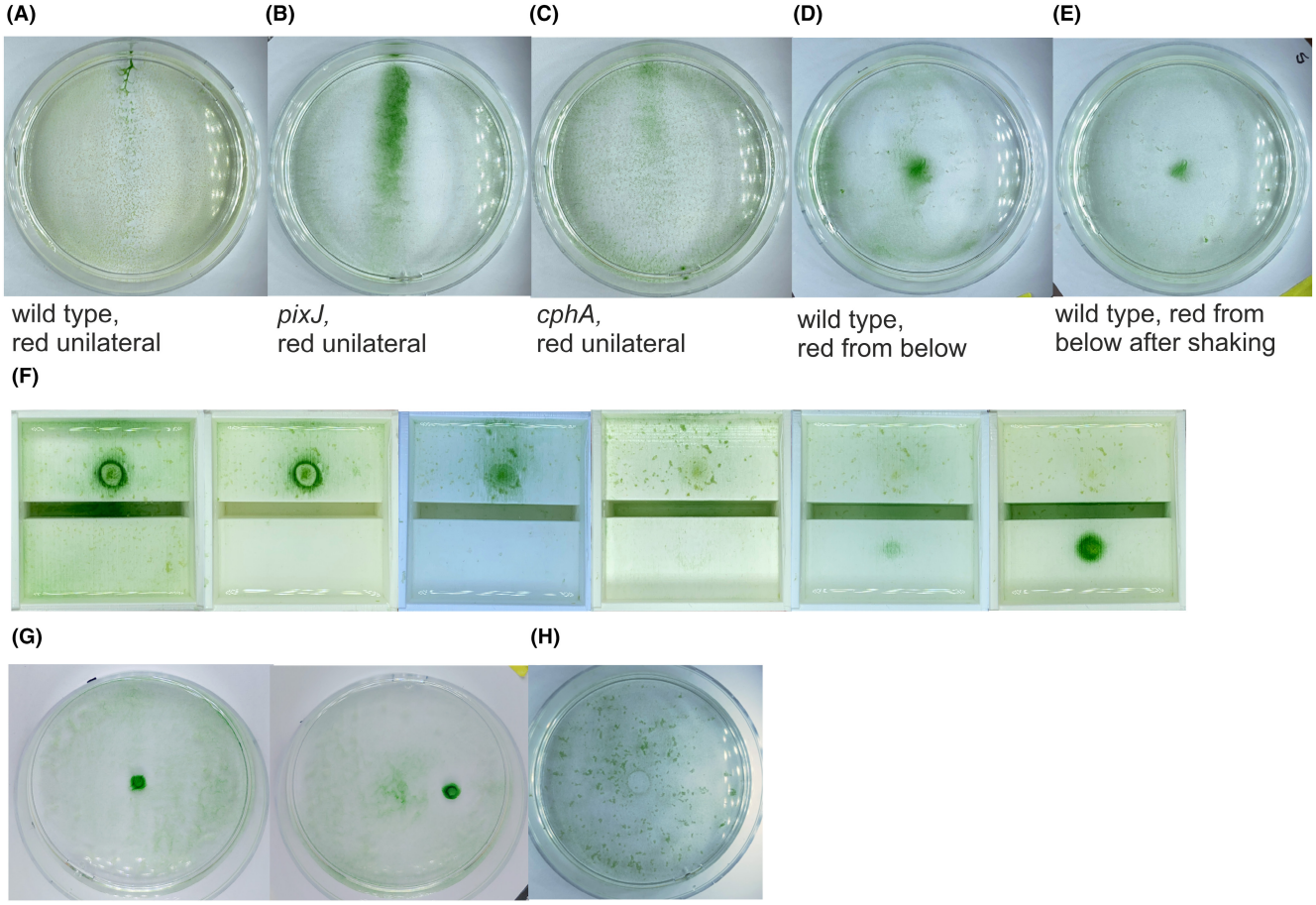

FIGURE 3 Phototaxis and photophobotaxis of *Phormidium lacuna*. (A–C) Phototaxis experiment, unilateral irradiation with red light coming from the upper side of the pictures (plates are horizontal, see Figure 1A,B), 10 μmol $m^{-2} s^{-1}$ for 2 days. (D, E) photophobotaxis experiment with wild type, red light from below, 10 μmol $m^{-2} s^{-1}$ for 2 days, before (D) and after (E) shaking. Note the reduction in the biofilm area. (F) Irradiation in a container with a ditch, outline as in Figure 1E,F. From left to right: after 24 h irradiation at position 1 with red light of 10 μmol $m^{-2} s^{-1}$ (note the ring formation); after removal of excess filaments in the container, LED at position 1 was switched off and LED at position 2 was switched on; 6 h after start of irradiation at second position; 24 h after switch on of second light; 48 h after switch on; 72 h irradiation at position 2. Experiment was repeated three times with qualitatively identical results. (G) Wild-type filaments irradiated as in d (left photo), and for another 2 days outside the center (right photograph). The experiment was repeated 10 times with same outcome. (H) example for ring formation with *pixJ* filaments irradiated in presence of 100 μM DCMU, red light from below, 10 μmol $m^{-2} s^{-1}$ for 2 days.

phototaxis, although the response was weak. Subsequent photophobotaxis experiments were performed with light shining perpendicular on the surface.

Filaments gather as a biofilm within illuminated areas by photophobotaxis

For photophobotaxis assays, a solution with filaments was poured into a Petri dish that was placed on a holder with a light-emitting diode. This LED shines light from below through the bottom of the Petri dish at the center of the solution (see outline in Figure 1C,D; see also Ref. 8). The standard illumination time was 2 days; however, under ambient light, the directional response could be observed after several hours. A biofilm with high filament density was formed within the illuminated area. A comparison before and after shaking provided an impression of the stability of the biofilm. Examples of red light irradiated wild type before and after shaking are shown in Figure 3D,E.

Irradiations at two positions

Biofilm stability was also evaluated by subsequent irradiation at diverse positions in the container. In one series of experiments, the filaments were first irradiated for 2 days in the center of a Petri dish and then for another 2 days at a position 1 cm outside the center of the Petri dish. After the first irradiation, a round biofilm was observed in the center, as expected (Figure 3G, left). After the second irradiation, the biofilm at the first position was lost, and another round biofilm was

formed at the second position (Figure 3G, right). The filaments had moved from the first to the second position.

Twitching motility is based on surface attachment. However, the oscillations of filaments in a liquid[8] led us to assume that filaments could also move forward in a liquid solution without surface contact. We therefore tested whether the filaments required a surface to move from one position to another. We constructed a container with LEDs at two positions and with a ditch in between (Figure 1E,F). To migrate from one position to the other, filaments could either move across the ditch, thereby losing surface contact, or migrate down and up the vertical walls of the ditch. The container was filled with filaments in the medium, and the LED on one side was switched on. After 24 h, a biofilm was formed at the LED position. Thereafter, the medium was replaced with fresh medium so that only the biofilm filaments remained and the second LED was switched on. After another 3 days, the filaments migrated to the second light spot. The filaments first disappeared in the ditch before appearing on the other side, where they moved toward the 2nd light spot (Figure 3F). There were no indications of movement across the ditch. The complete migration from the first to the second position took 3 days, and direct movement took approximately 2 days, indicating that filaments needed longer because they moved down and up the walls. This experiment demonstrated that the filaments could move forward only through surface contact.

Time lapse recordings demonstrated that filaments are captured in the light spot

In order to find out the mechanism how the filaments move to the light, we established time-lapse recordings under red and infrared light. We used a red LED to induce photophobotaxis. The LED-light was also used for the recordings by the camera. The area surrounding the red light (dark area) was illuminated by infrared light, which had no impact on the filament responses. The following observations were made from 11 videos, each covering 8–10 h. An example is shown in Video S1.

All filaments moved along their longitudinal axes in random directions (Video S1). Typically, the filaments switched their moving direction from forward to backward on a minute timescale. In earlier experiments, wherein movement was studied on agar surfaces, the same back and forth movement was observed,[8] but in the present experiments, the reversion frequency was lower and the movement speed was faster. Two hours after onset of light, an increased filament density was observed in the illuminated area and the filament density increased further in the subsequent hours. This increase was anticipated from

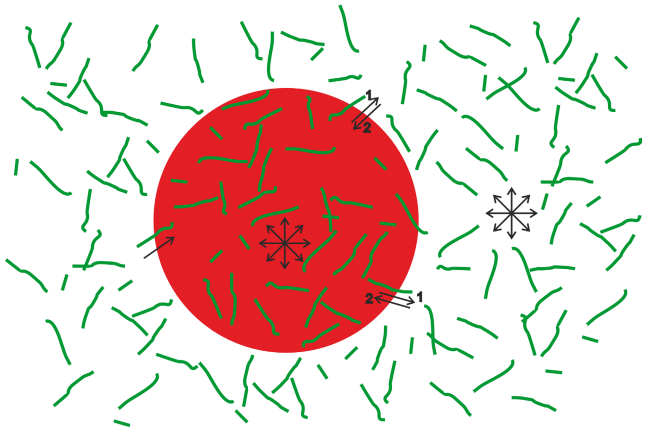

FIGURE 4 Photophobotaxis light capture of *Phormidium lacuna*. Cartoon to summarize results of time lapse video recordings. The red circle stands for the illuminated area, filaments are drawn in green. The arrows indicate movement directions, the multi-arrows symbolize random movements within and outside the illuminated area. Filaments that cross the edge between light and dark from the lighted side (arrows denoted 1) turn their movement direction and return into the illuminated area (arrows denoted 2).

the steady-state experiments. In the time-lapse videos it became clear that also all filaments within the illuminated area moved, although biofilm formation suggested that the filaments became immobile. A biofilm is thus formed by a dynamic filament network with multiple transient connections to the plastic surface.

When a filament moved from the illuminated area to the edge of this area and crossed the light–dark border, it reverted its movement direction and moved back into the illuminated area. Many examples for such reversions can be seen in Video S1. Due to this effect, the filaments can move from the dark area into the illuminated area, but not in the other direction, as also outlined in the cartoon of Figure 4. In one video, we counted 43 light–dark crossings that resulted in a reversion back to the light, and the estimated mean time that the filament tip was outside the illuminated area was 110 ± 10 s (mean ± SE). A large number of reversions was probably overseen because only a fraction of the filaments was in focus. In all 11 videos, we found no filament that escaped from the illuminated area. Thus, photophobotaxis is based on movements in random directions and a reversion of movement upon the light–dark transition back to light.

Irradiation from below and above at different wavelengths

In most settings, the filaments were irradiated from below, which is the preferred direction for time lapse microscope studies. However, in the natural environment, the sunlight

comes rather from above or from the side. We now investigated the response of *P. lacuna* toward light from above and compared it with the response to light from below. We used LEDs of six different wavelengths between 467 and 750 nm to get information about the spectral sensitivity of the response. The distances between LED and filaments were larger than in the other experiments, resulting in illuminated areas of 65 mm^2. The results are depicted in Figure 5. With the wild-type filaments, irradiation from above and below yielded comparable biofilm areas. Blue, green, yellow, and far-red (700 nm) light produced 30–60 mm^2 biofilm areas. The biofilm area under red light from below with 40 mm^2 was also within this range, whereas irradiation with red light from above yielded a biofilm area of only 20 mm^2. The difference between the red light from above and below was significant (MW test). With long-wavelength far-red light (750 nm), no response was found. The photophobotaxis response of the *cphA* mutant was comparable to that of the wild type, and the blue, green, red, and far-red biofilm areas were between 25 and 35 mm^2. However, under two illumination conditions, yellow light from below and red light from above, large biofilm areas of approximately 130 and 180 mm^2, respectively, were obtained; the filaments accumulated inside and outside the illuminated area. Most likely, filaments have escaped the light, but remained next to the light. The large-area effect was specific to *cphA*, and the differences between the wild type and *cphA* were significant (MW test). After shaking, the *cphA* biofilm area was zero in eight out of 12 cases and that of the wild type was zero in 5 out of 12 cases. The attachment of *cphA* to the surface was thus weaker than that of the wild type.

Results with the *pixJ* mutant were different from those of the other strains, as also 750 nm light induced a clear response (Figure 5). This light was inactive in wild type and *cphA*. With light from above, the biofilm areas were larger than those of the wild type for most wavelengths. Light from below between 467 and 700 nm induced weaker responses in *pixJ* as compared to light from above and as compared to wild type. There was thus a clear effect of light direction on the extent of photophobotaxis. Shaking diminished the *pixJ* biofilm areas to a smaller extent than in the wild-type or *cphA* (Figure 5).

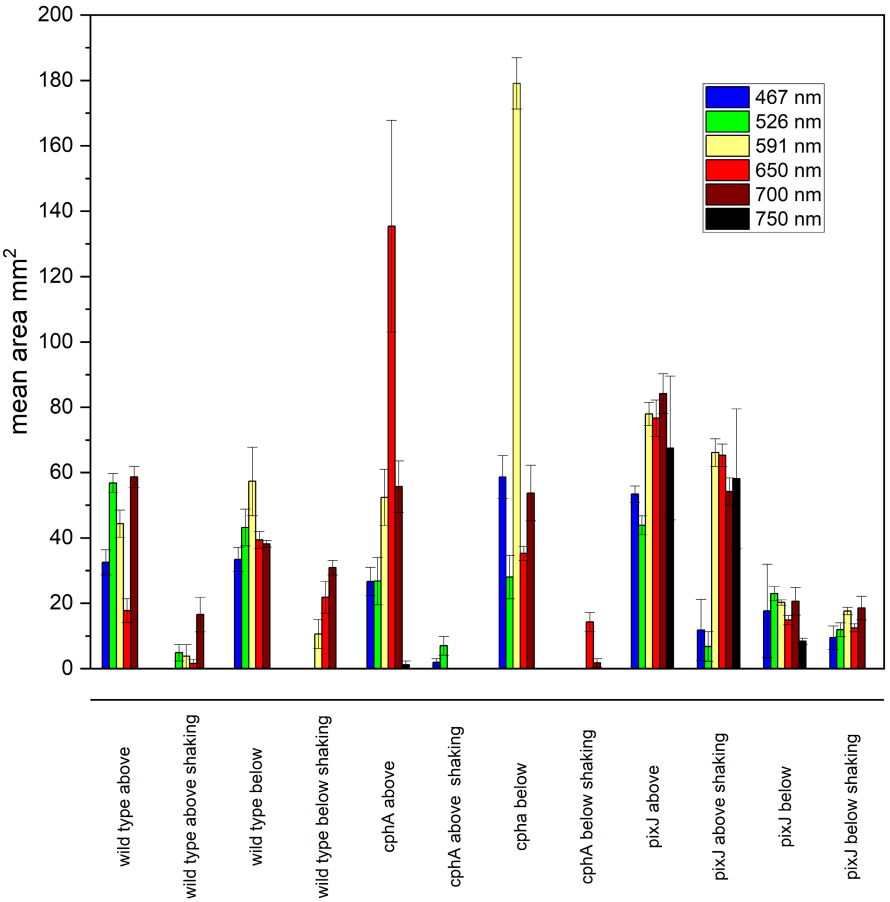

FIGURE 5 Photophobotaxis of *Phormidium lacuna* wild-type, *cphA* and *pixJ* irradiation with different wavelengths from above and from below. Mean values ± SE of 7–10 independent measurements. The illuminated area was 65 mm^2 for both directions of irradiation, the duration of illumination was 2 days. Light intensities were 10 $\mu mol\, m^{-2} s^{-1}$, wavelengths are given in the panel.

Photophobotaxis between 467 and 750 nm and over 4 decades of light intensity

We then tested photophobotaxis of wild type, *pixJ*, and *cphA* at diverse light intensities between 0.01 and 10 µmol $m^{-2} s^{-1}$ with light from below, the irradiated area was 25 mm^2. The same six wavelengths as in Figure 5 were utilized. The variation in light intensities and the more focused light beam provided additional information about the effect and about mutant phenotypes. The results are represented in Figure 6, and the significance of the differences between the wild type and mutants are represented in Table 1. All wavelengths induced a response in all three strains, at least at high light intensities. Under red light (650 nm), a typical intensity response curve over the range of four decades was obtained for wild-type filaments. The mean biofilm area at the light spot was 3 mm^2 at 0.01 µM $m^{-2} s^{-1}$ and

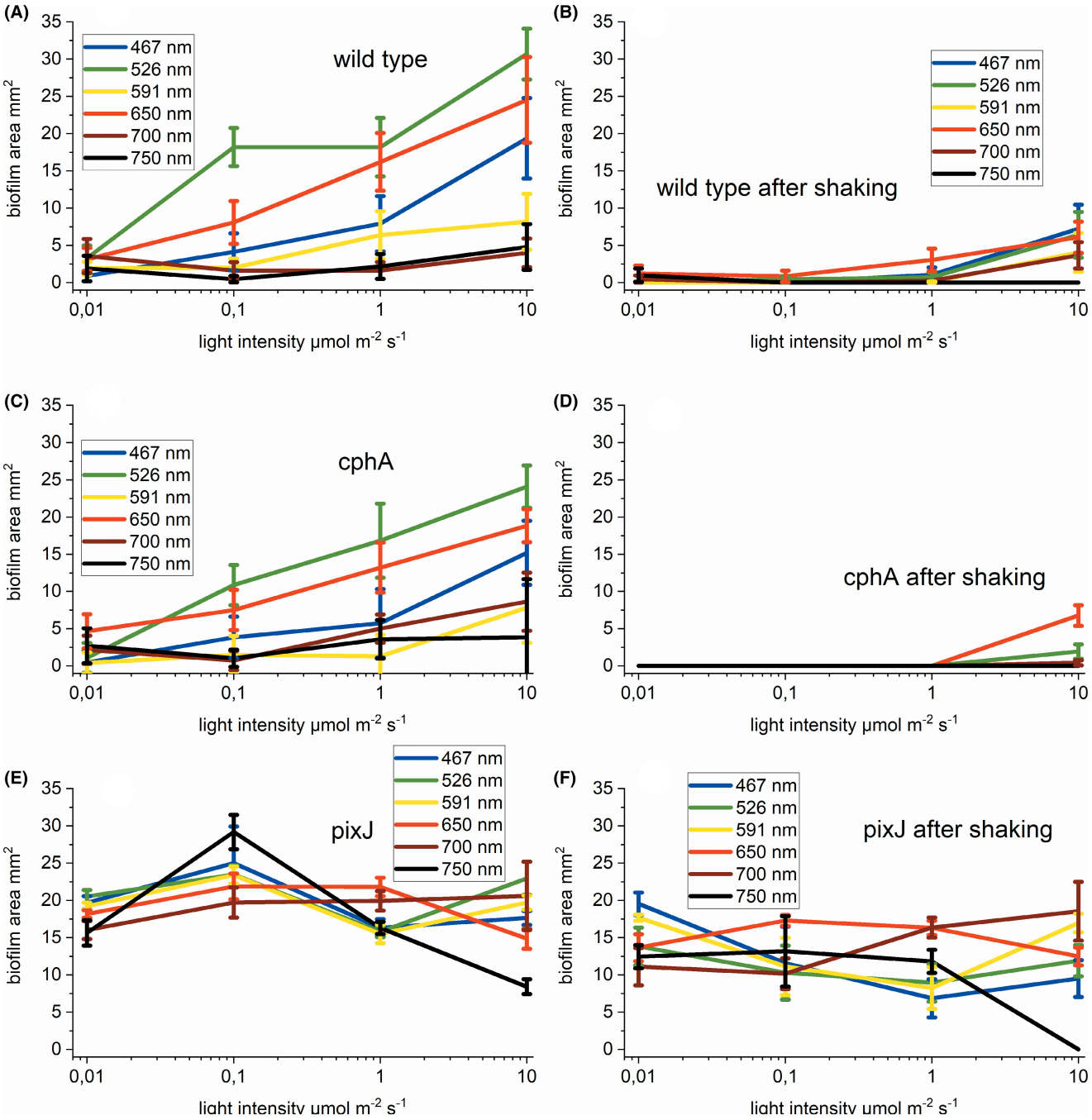

FIGURE 6 Photophobotaxis with *Phormidium lacuna* wild-type, *cphA* and *pixJ*, irradiations with different wavelengths and light intensities. Irradiation from below for 2 days. The illuminated area was 20 mm^2. Mean values ± SE of 7–12 independent measurements for each data point. Significances are given in Table 1.

TABLE 1 Significance of differences between strains based on the data shown in Figure 6.

Before shaking					
		μmol m^{-2} s^{-1}			
	Wavelength	0.01	0.1	1	10
wt/cphA	467 nm				
wt/pixJ	467 nm	*	*	*	
pixJ/cphA	467 nm	*	*	*	
wt/cphA	526 nm				
wt/pixJ	526 nm	*	*		
pixJ/cphA	526 nm	*	*		
wt/cphA	591 nm				
wt/pixJ	591 nm	*	*	*	*
pixJ/cphA	591 nm	*	*	*	
wt/cphA	650 nm				
wt/pixJ	650 nm	*	*		
pixJ/cphA	650 nm	*	*	*	
wt/cphA	700 nm				
wt/pixJ	700 nm	*	*	*	*
pixJ/cphA	700 nm	*	*	*	
wt/cphA	750 nm				
wt/pixJ	750 nm	*	*	*	
pixJ/cphA	750 nm	*	*	*	
wt/cphA[1]	All wavelengths	nt	nt	nt	*
After shaking					
		μmol m^{-2} s^{-1}			
	Wavelength	0.01	0.1	1	10
wt/cphA	467 nm				*
wt/pixJ	467 nm	*	*	*	
pixJ/cphA	467 nm	*	*	*	*
wt/cphA	526 nm				
wt/pixJ	526 nm	*	*	*	
pixJ/cphA	526 nm	*	*	*	*
wt/cphA	591 nm				
wt/pixJ	591 nm	*	*		*
pixJ/cphA	591 nm	*	*	*	*
wt/cphA	650 nm				
wt/pixJ	650 nm	*	*	*	
pixJ/cphA	650 nm	*	*	*	
wt/cphA	700 nm				*
wt/pixJ	700 nm	*	*	*	*
pixJ/cphA	700 nm	*	*	*	*
wt/cphA	750 nm				
wt/pixJ	750 nm	*	*	*	
pixJ/cphA	750 nm	*	*	*	
wt/cphA	All wavelengths	*			

Note: Same wavelengths were compared between strains. Significance was determined by Mann Whitney test.[25] * stands for error of probability of $p < 0.05$. We did not distinguish between $p < 0.01$ and $p < 0.05$. In the last line under "before shaking," 10 μmol m^{-2} s^{-1} of all wavelengths were compared between wild type and *cphA*. In the last line under "after shaking," irradiations between 0.01 and 1 μmol m^{-2} s^{-2} of all wavelengths were compared between wild type and *cphA*. For each wavelength, all single values were normalized to the mean values out of both strains of this wavelength.

Abbreviation: nt, not tested.

increased continuously to 24 mm^2 at 10 μmol m^{-2} s^{-1}. The green light (526 nm) intensity-response curve was slightly above that of red light, but otherwise comparable; at 10 μmol m^{-2} s^{-1} the area was 31 mm^2. The responses to blue (467 nm) and yellow light (591 nm) were weaker than those to red or green light, and the biofilm areas were 14 and 8 mm^2 at 10 μmol m^{-2} s^{-1}, respectively. With far-red light at 700 and 750 nm, only very weak responses with mean biofilm areas of 3 mm^2 or less were obtained. Shaking reduced the biofilm areas in these wild-type experiments more than in comparable earlier experiments[8] or in experiments described below. The largest areas after shaking were 6.4 and 6.1 mm^2 for green and red light at 10 μmol m^{-2} s^{-1}, respectively. The reason for this difference was probably due to the diverse preculture conditions used. However, qualitative differences between the mutants (see below) and the wild type remained unaffected.

Biofilm formation is affected in *cphA* mutants

The *cphA*-mutant biofilm areas were smaller than those of the wild type at all wavelengths, except for 700 nm (Figure 6). For single wavelengths, the differences between the wild type and *cphA* were not significant (MW), but when data at 10 μmol m^{-2} s^{-1} under the inclusion of all wavelengths were taken, the values of *cphA* were significantly (MW test) smaller than those of the wild-type (Table 1). This finding aligns an earlier study, in which the *cphA* biofilm under red light was significantly (MW test) smaller than that of the wild type.[8]

After shaking, *cphA* and the wild-type were significantly (MW) different for 10 μmol m^{-2} s^{-1} at 700 and 467 nm. For *cphA*, in all treatments up to 1 μmol m^{-2} s^{-1} intensity, no filaments remained attached after shaking. When a significance test was performed including all data between 0.01 and 1 μmol m^{-2} s^{-1}, the difference between *cphA* and wild type was significant (MW) (Table 1). The reduced attachment of *cphA* compared with the wild type is again in line with an earlier study[8] and other experiments reported above and below.

PixJ is a negative photophobotaxis regulator

The responses of *pixJ* mutants were unexpected. The proposed role of PixJ as a receptor for phototaxis suggested a weaker response of the mutant than that of the wild type. However, under most conditions, the *pixJ* responses were stronger than those of the wild type

(Figure 6 and Table 1 for significant differences). The biofilm area of *pixJ* was always between 15 and 25 mm^2. The lowest light intensity that was used, 0.01 $\mu mol\ m^{-2}\ s^{-1}$, is so weak that the light could not or barely be seen by eye. We expected this light to be too weak to induce strong photophobotaxis. However, the responses of *pixJ* to 0.01 $\mu mol\ m^{-2}\ s^{-2}$ of any light color were in the same range as the responses to 10 $\mu mol\ m^{-2}\ s^{-1}$. Additionally, the responses at 700 and 750 nm at low and high intensities, respectively, were unexpectedly high. The 750 nm response was stronger at 1 $\mu mol\ m^{-2}\ s^{-1}$ than at 10 $\mu mol\ m^{-2}\ s^{-1}$. This reduction at high light intensities is probably the result of overstimulation. In 750 nm light, the response of *pixJ* at low light intensities was 1000–10,000 times more sensitive than that of the wild type, as 750 nm light with 0.01 $\mu mol\ m^{-2}\ s^{-1}$ yielded a much larger response in *pixJ* than the strongest 750 nm light with 10 $\mu mol\ m^{-2}\ s^{-1}$ in wild type. These data show that PixJ is a negative photophobotaxis regulator in *P. lacuna*. The weak 0.01 $\mu mol\ m^{-2}\ s^{-1}$ light is probably too weak to induce significant PixJ photoconversion. In this low-intensity range, the inhibitory effect of PixJ was therefore light-independent.

After shaking, *pixJ* biofilm areas were usually larger than those of wild type (Figure 6). At 10 $\mu mol\ m^{-2}\ s^{-1}$ intensity, wild type and *pixJ* were significantly different (MW) before and after shaking in 4 and 3 of 6 colors, respectively. At 1 $\mu mol\ m^{-2}\ s^{-1}$, wild type and *pixJ* biofilms were significantly different before and after shaking in 3 and 5 colors, respectively. We did not perform a more detailed statistical analysis of such differences. However, the overall impression was that *pixJ* had the strongest attachment to the surfaces of all three strains.

Photosynthesis blockers inhibit photophobotaxis

The broad spectral range of photophobotaxis indicated the possible role of photosynthesis in this effect, because the spectral range of photoreceptors is considerably narrower. Therefore, we investigated the effects of 3-(3,4-dichlorophenyl) 1,1-dimethylurea (DCMU) and methylviologen (MV) on photophobotaxis. DCMU binds to the D2 subunit of PS II and blocks the electron transfer chain to plastoquinone B (PC_B),[34] and MV transfers PS I electrons to water.[35]

Before testing for photophobotaxis, we performed growth assays using *P. lacuna* wild type to determine the relevant concentration ranges (Figure 7). In these assays, DCMU inhibited growth partially at a concentration of 0.01 µM and almost completely at 0.1 µM (Figure 7 left panel). The 1% ethanol control reduced growth to approximately 2/3. The 1000 µM DCMU solution also contained 1% ethanol, the other DCMU solutions 10× or 100× less, and the reduction in growth was therefore largely a DCMU effect. There was no significant effect of MV on growth for concentrations of 0.1–1 µM, whereas 10 µM inhibited

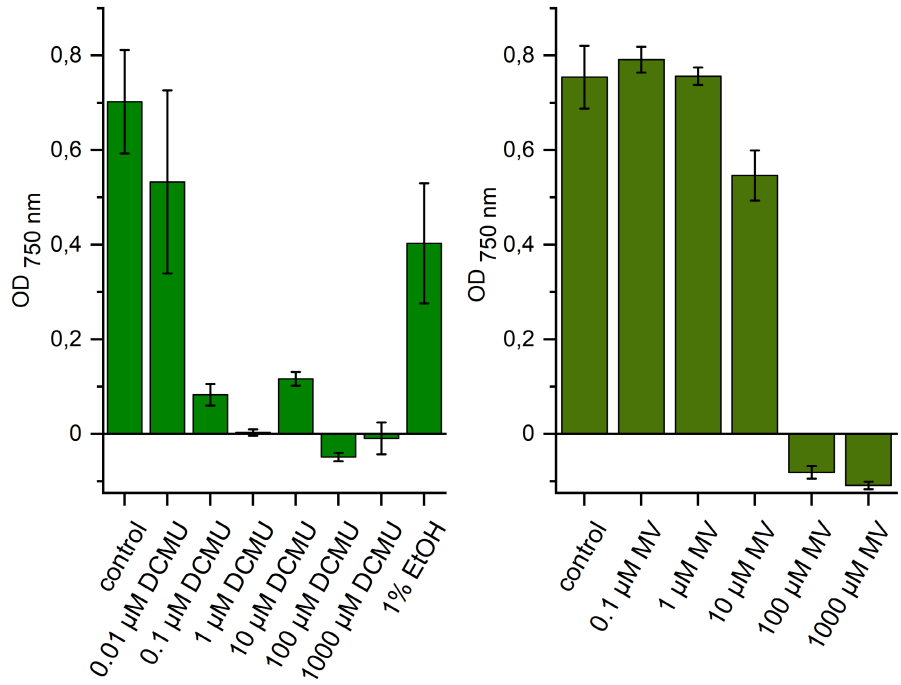

FIGURE 7 Growth of *Phormidium lacuna* wild type in presence of DCMU or MV. Cultures with a start $OD_{750\ nm} = 0.1$ were cultivated for 1 week in the growth room under agitation. Mean values of 3 experiments ± SE. [Color figure can be viewed at wileyonlinelibrary.com]

growth slightly. At 100 and 1000 µM, almost complete or complete inhibition was observed, respectively.

DCMU inhibits photophobotaxis in a specific manner

As in the growth experiments, solutions containing DCMU contained 0.01%, 0.1%, or 1% ethanol. We therefore made controls with 0.1% and 1% ethanol for photophobotaxis and motility experiments. With 1% ethanol, photophobotaxis was reduced from 23 to 14 mm^2 (Figure 8). With 0.1% ethanol, there was no significant effect on photophobotaxis. In all strains, the biofilm that was formed in 1% ethanol was stable after shaking, unlike under conditions without ethanol. Ethanol can increase biofilm formation in other bacteria.[36] In the DCMU experiments, we concluded that the inhibitory effects were predominantly based on the inhibitor and not on ethanol.

The range of 0.01–1000 µM DCMU was tested for photophobotaxis of wild type, *cphA*, and *pixJ* in red light of 10 µmol $m^{-2} s^{-1}$ (Figure 8). In wild-type filaments, up to 10 µM DCMU had almost no effect on photophobotaxis. At 100 and 1000 µM DCMU, photophobotaxis was partially and completely inhibited, respectively. The inhibition of photophobotaxis occurred thus at higher concentrations as the inhibition of growth. The high concentration of DCMU required for growth inhibition could indicate that a small fraction of uninhibited PS II is sufficient to induce photophobotaxis, but could also point to an unspecific effect. To distinguish between both possibilities, the filaments from the photophobotaxis assays were subsequently subjected to motility tests. These experiments showed that all filaments were motile up to 1000 µM DCMU, although in case of the mutants, a reduction was observed with increasing DCMU concentrations (Figure 9). With the 7 µm min^{-1} migration speed observed with wild-type filaments at 1000 µM DCMU, a visible fraction of filaments

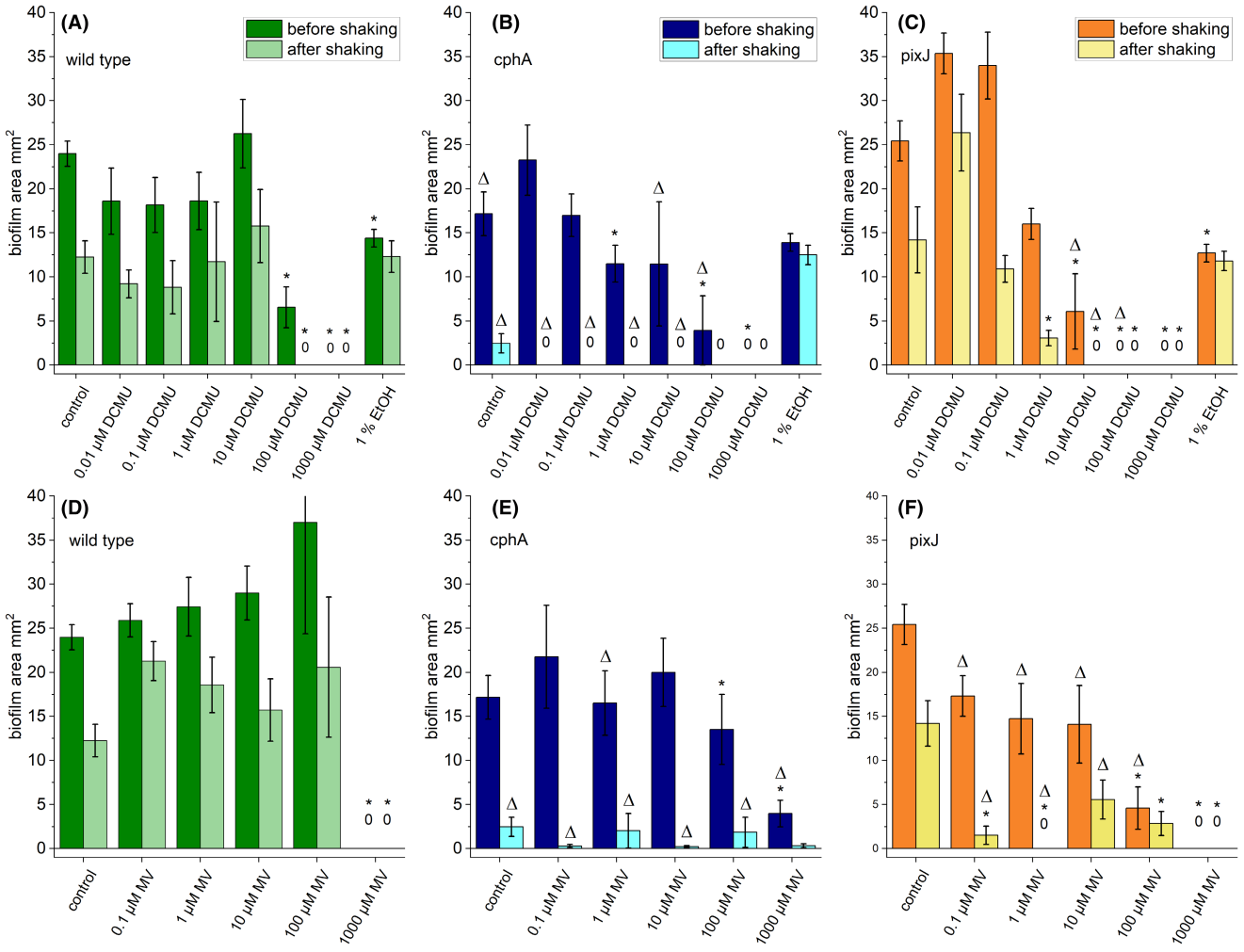

FIGURE 8 Photophobotaxis of *Phormidium lacuna* wild type, *cphA* and *pixJ* in presence of DCMU or MV. All samples were irradiated for 2 days with red light of 10 µmol $m^{-2} s^{-1}$. Strains are given in the panels; inhibitor compound is given in the *x*-axis legend. Mean values ± SE of 10 independent measurements each.

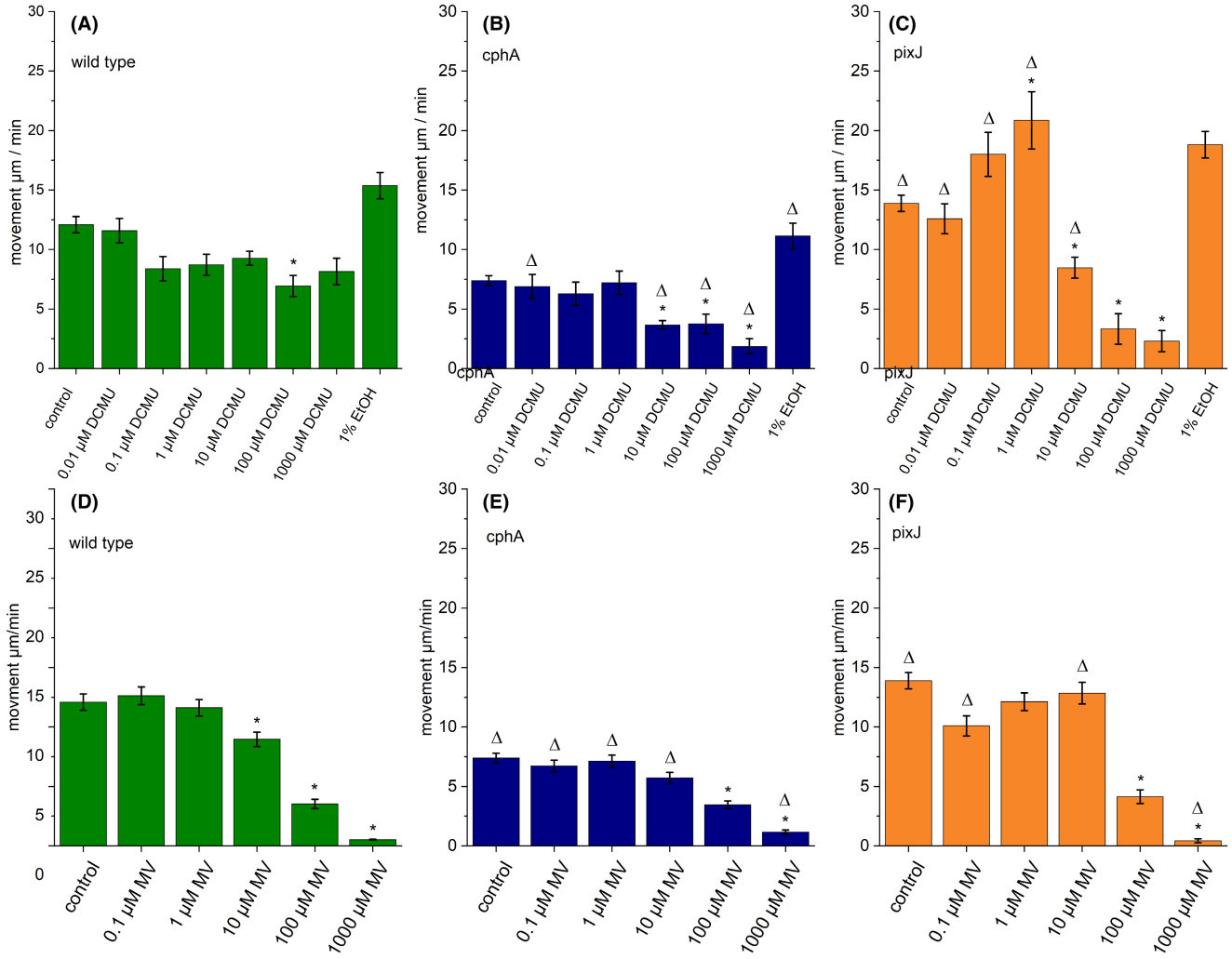

FIGURE 9 Motility of *Phormidium lacuna* after treatment with DCMU or MV. Mean values ± SE of 50 or more single measurements for each bar. After 2 days photophobotaxis (Figure 7), a fraction of the filaments was transferred to agar plates and the motilities estimated as described in the Materials and Methods section. Asterisks (*) indicate significant differences between control and sample, the delta symbol (Δ) indicates significance of difference between wild type and respective strain. Significance was estimated by the non-parametric Mann–Whitney test and $p < 0.05$.

could reach the light zone, sind with 12 µm min^{-1} of the control, a high portion of filaments entered the light The 2 µm min^{-1} obtained with the mutants at 1000 µM DCMU would be equivalent to a distance of 5 mm in 2 days. Some accumulation of filaments in the light cone should have been detected if light sensing were functional.

The biofilm areas in the *cphA* control experiments without DCMU were significantly smaller than those in the wild type. Otherwise, the *cphA* DCMU concentration pattern was comparable to that of the wild type. After shaking, the biofilm was lost in the *cphA* samples. Differences between wild type and *cphA* were significant at 0, 0.01, 0.1, 1, and 10 µM. This finding emphasizes the effect of CphA on biofilm stability.

The *pixJ* biofilm areas were larger than the wild type at 0.01 and 0.1 µM DCMU and larger than the control (Figure 8), but the differences were not significant. However, at 10 and 100 µM DCMU, the biofilm areas were significantly smaller than those of the wild type, as if PixJ protected the wild type against DCMU. With 100 µM DCMU, we observed that *pixJ* filaments moved out of the illuminated area and formed a ring surrounding this area (Figure 3H, Table 2). (For such cases, the biofilm area was considered 0.) This ring formation was observed in all 10 *pixJ* experiments with 100 µM DCMU, whereas for the wild-type, only 2 out of 10 followed this pattern. For *cphA*, one open ring was observed (Table 2).

We tested for correlations between motility/photophobotaxis or growth/photophobotaxis by the linear fit function of the Origin software. These analyses are summarized in Table 3 and graphically presented for two examples in Figure 10. If photophobotaxis were directly dependent on motility, there should be a high correlation between both parameters. A significant correlation between

TABLE 2 Ring formation in experiments with DCMU and MV.

	0	0.01 μM	0.1 μM	1 μM	10 μM	100 μM	1000 μM
wt DCMU	–	–	–	–	–	2	–
cphA DCMU	–	–	–	–	3	1	–
pixJ DCMU	–	–	–	1	2	10	–
wt MV	–	–	–	–	–	10	10
cphA MV	–	–	–	–	–	8	10
pixJ MV	–	–	–	–	–	7	6

Note: See Figure 3H for ring formation. The numbers indicate the number of Petri dishes in which rings were observed (out of 10 circles).

TABLE 3 Linear fit analysis with DCMU and MV data.

		Photophobotaxis			Motility		
		Wild type	*cphA*	*pixJ*	Wild type	*cphA*	*pixJ*
DCMU							
Growth	Wild type	No 0.02	Yes 0.43	No 0.21	Yes 0.61	No 0.28	No 0.11
Motility	Wild type	No 0.11					
	cphA		Yes 0.31				
	pixJ			No 0.40			
MV							
Growth	Wild type	No 0.02	No 0.60	Yes 0.88	Yes 0.96	Yes 0.89	Yes 0.80
Motility	Wild type	No 0.02					
	cphA		Yes 0.88				
	pixJ			Yes 0.81			

Note: Data pairs for growth/motility, growth/photophobotaxis and motility/photophobotaxis for the different inhibitor concentrations were subjected to the test. "Yes" indicates that the slope of the curve is significantly different from zero, "no" indicates that the slope is not significantly different. The number gives the correlation coefficient *R*-square which can be between 0 and 1 (no and high correlation).

photophobotaxis and motility was not found for wild type or *pixJ*, but between motility and growth of the wild type. The correlation for *cphA* between motility and photophobotaxis of *cphA* was significantly different from zero, but the correlation coefficient of 0.43 was low. As a summary of all DCMU results and these comparisons one may conclude that there were many conditions under which the filaments were motile but where photophobotaxis was blocked. We conclude from these analyses that photosystem II could act as photosensor of photophobotaxis.

DCMU inhibits *Synechocystis* sp. PCC 6803 photophobotaxis

To determine how the photophobotaxis of other species is affected by DCMU, we performed studies using the unicellular cyanobacterium, *Synechocystis* sp. PCC 6803. We used the same approach as for *P. lacuna*: a 5 mm LED irradiated a cellular culture in a Petri dish from below (Figure 1C,D). As depicted in Figure 11, the cells accumulated in the illuminated area 2 days after the onset of light. The cells in the center remained connected by a slimy matrix. With 0.01 and 0.1 μM DCMU, a comparable photophobotactic response was obtained. With 1 μM DCMU and higher concentrations, no photophobotaxis was seen. The experiment was performed four times with similar outcomes. *Synechcystis* sp. PCC 6803 underwent photophobotaxis, and the response was inhibited by DCMU at much lower concentrations than *P. lacuna* photophobotaxis.

Inhibition by MV is unspecific

Methylviologen (MV) blocks the photosynthetic electron chain of PS I. *P. lacuna* growth was inhibited at 100 μM MV and more, that is, at much higher concentrations as compared to DCMU (Figure 8, correlation data are also presented in Table 3). The photophobotaxis of wild-type filaments was not affected by up to 100 μM MV, a concentration at which growth was already inhibited (Figure 7). Only at the highest concentration of 1000 μM, no photophobotaxis response was observed. As motility was also inhibited at this concentration (Figure 9), we assumed that the cells did not survive. Thus, *P. lacuna* responds differently to MV than to DCMU. We conclude that PS I

inhibition does not directly affect photophobotaxis of the wild type in a specific manner. However, ring formation was observed for all strains at 100 µM MV.

The *cphA* biofilms in the MV experiments were smaller than the wild-type biofilms (Figure 8), although only at 1 µM these differences were significant. We observed that shaking reduced biofilm formation in the *cphA* strain more than in the other two strains. For *pixJ*, an unexpected response pattern was observed in the MV experiments. In most previous experiments, *pixJ* biofilms were larger than or equal to wild-type biofilms, whereas in the MV experiments, the *pixJ* biofilms were significantly smaller than wild-type biofilms in all cases where MV was present. With increasing MV concentrations up to 100 µM, the biofilm areas increased in the wild type but decreased in *pixJ*. PixJ appeared to protect filaments against photophobotaxis inhibition by MV.

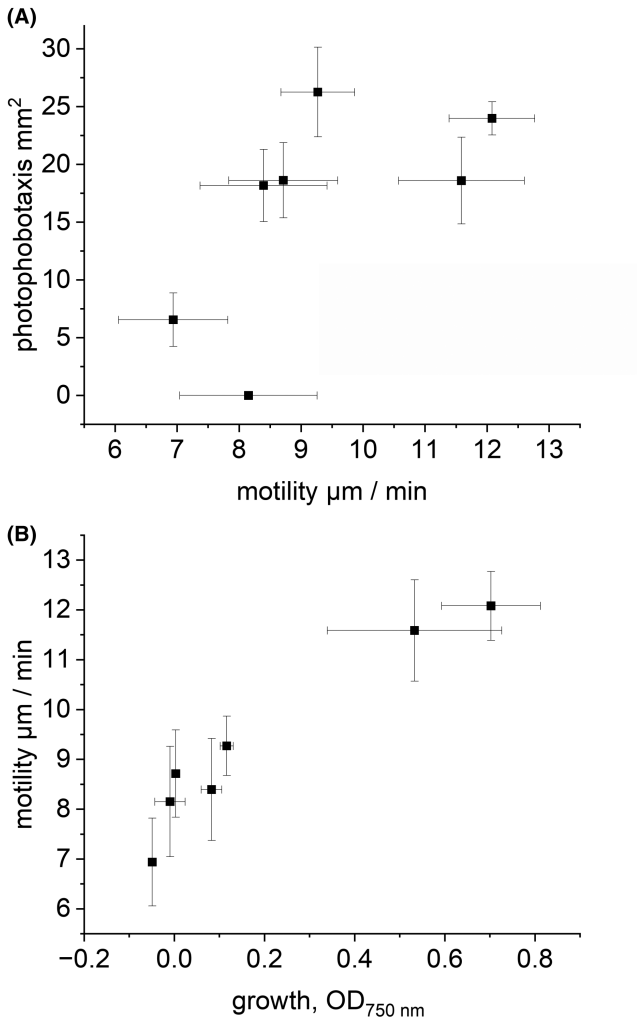

FIGURE 10 Data of Figures 8 and 9 are plotted against each other.

DISCUSSION

By twitching motility, cyanobacteria can move toward light if the light is weak, or away from light if the light is too strong. In this study, movement toward unilateral light, phototaxis, and toward a light spot, photophobotaxis, were observed. The latter response was further characterized by different wavelengths, light intensities and by inhibitor studies. It has been demonstrated earlier that type IV pili are involved in the gliding movement of *P. lacuna* photophobotaxis.[8] Here, we demonstrate that movement toward light always proceeds along the surface and not through the liquid medium (Figure 3F), although filaments can move against each other in a liquid through oscillatory movements.[8]

We observed by time lapse recordings (Video S1) that filaments accumulate in the light by a combination of random movement and the reversion of movement upon light-to-dark transition. By random movement, a filament can find the light and by the reversion, it remains in the light (Figure 4). The reversion must be triggered by a temporal or spatial difference of the light signal at the level of each filament. Although it takes several hours for an enrichment of filaments in photophobotaxis to be observed, a phobic change in movement direction takes place within approximately 2 min, the time when a filament reaches out of the light until it returns to the light. The long time that it takes until the biofilm is formed results from the distance between the original positions of the filaments and the light and the fact that the movement is not straight but in random directions.

Whereas the light trap model can explain photophobotaxis under standard conditions, some experimental

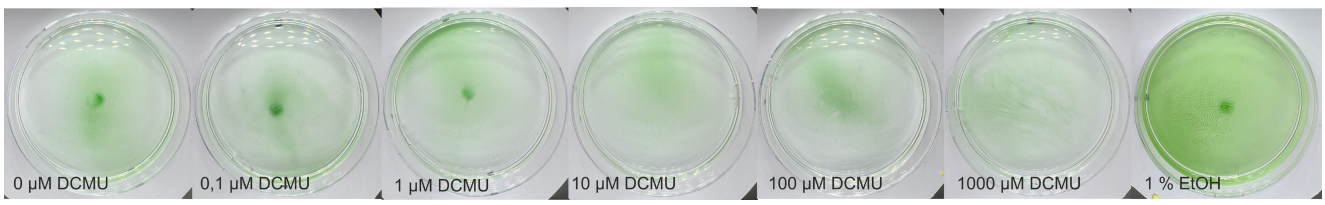

FIGURE 11 *Synechocystis* sp. PCC 6803 photophobotaxis with varying concentrations of DCMU. The cells were brought into the 5 cm Petri dishes and placed on a 5-mm red LED with 10 µmol $m^{-2} s^{-1}$ for 2 days. The DCMU concentrations are given in each panel. The left panel shows a dark control without DCMU. The experiment was repeated four times with qualitatively same outcome.

findings require additional assumptions and more research for clarification. Under some conditions, biofilm areas were found that are larger than the illuminated area. An explanation could be that outer filaments exit the illuminated area as there is not enough space in the illuminated area. Because the light trap model suggests always movement up to the light–dark border, biofilm areas that are smaller than the illuminated area are also not compatible with the model. These small biofilms are obtained at low light intensities. Possibly, the relevant photoreceptor is not activated enough by the weak light. This could allow an escape of a fraction of the filaments from the light field. Additionally, filaments in the center of the illuminated area must stick together such that the biofilm does not cover the entire light area. Ring formation (Table 2) does also not fit with the light trap model. If we assume that filaments change their movement direction upon light–dark transition and also dark–light transition, we can explain such a pattern. Note that in other experiments, not reported here, we observed ring formation more frequently, especially under very strong light. A switch between positive and negative light responses that is dependent on the light intensity is often found in phototaxis and many other responses.

There is a general mechanistic difference between photophobotaxis and the phototaxis of single-celled cyanobacteria. The basis for photophobotaxis is a light intensity gradient along the filament or a gradient over time, and the basis for phototaxis is a light intensity gradient within a single cell along the light direction. Effects that are related to the light direction were also found for *P. lacuna*: light from above and light from below gave different results, and unilateral light-induced phototaxis also in *P. lacuna*.

If the filaments gather in a light area, they form a biofilm that is resistant to shaking. However, the biofilm is a dynamic formation of filaments. We observed that not only those filaments outside a biofilm but also all filaments within a biofilm moved steadily. Moreover, in experiments, wherein the samples are subsequently irradiated at two different positions (from below), the filaments moved from the first to the second light spot, indicating that they were not irreversibly attached to the first position (Figure 3F,G). The biofilm must result from an interfilamentous network formed as a consequence of higher filament density. Interconnected filaments bind to the surface by multiple transient contacts.

CphA is involved in biofilm formation

The major characteristics of the *cphA* mutant were its reduced biofilm area in photophobotaxis and its reduced binding to the irradiated area under several conditions (Table 4). Both effects are likely coupled. The reduced biofilm area of *cphA* may be due to reduced attachment to the surface. If biofilm stability is induced by light via CphA in the wild type, one would expect a dependency of biofilm stability on the wavelength, for example, strong binding under red light, the maximum of phytochrome absorbance, and weak binding under green light, which is not absorbed by phytochromes. Such an effect was not observed in the wild-type *P. lacuna*. Moreover, in *pixJ* mutants, very low light induced significant biofilm formation. CphA appears to affect pili attachment in a light-independent manner.

TABLE 4 Phenotype of *cphA* mutant.

Photophobotaxis: smaller biofilm as compared to wild type	Figures 5, 6 and 8
No or weak attachment to surface after photophobotaxis and shaking	Figures 5, 6 and 8
Reduced motility after photophobotaxis in DCMU, MV	Figure 9

The gene next to *cphA* and the response regulator gene encodes a multidomain protein (Figure 2A). According to domain predictions, the protein comprises a PAS, GGDEF, and an EAL domain. The GGDEF domain catalyzes the formation of the second messenger c-di-GMP, and the EAL domain catalyzes c-di-GMP degradation.[37] c-di-GMP is often involved in regulating cell adhesion and biofilm formation by cyanobacteria and other bacteria.[37] Several links between phytochromes and GGDEF/EAL have been reported in bacteria. The cyanobacterial phytochrome-like protein Cph2 has two GGDEF domains and one EAL domain[38] while a phytochrome from *Rhodobacter sphaeroides* has both GGDEF and EAL domains.[39] The *cphA* phenotype suggests that CphA regulates either diguanylate cyclase activity or its expression in *P. lacuna*. Another explanation could be that *cphA* gene interruption affects diguanylate cyclase expression level. However, we would presently rule out this possibility as the di-guanylate cyclase gene is separated by a 300 bp non-coding sequence from the 3′ end of the response regulator gene (Figure 2A) and is thus expressed separately from CphA.

PixJ is a negative photophobotaxis regulator

In other cyanobacteria, PixJ is often considered a phototaxis photoreceptor, but in *P. lacuna*, PixJ does not function as a light-direction sensor. In the *pixJ* mutant, photophobotaxis was enhanced compared to that in the wild type under low light intensities and far-red light at 700 and 750 nm (Table 5). Therefore, PixJ acts as a negative regulator for photophobotaxis. According to the PixJ

TABLE 5 Phenotype of *pixJ* mutant.

Response to unilateral light stronger than wild type or *cphA*	Figure 3B
Significant photophobotaxis at low light 0.01 μmol $m^{-2} s^{-1}$	Figure 6
Significant photophobotaxis with 700 nm and 750 nm light	Figures 5 and 6
Ring formation with 100 μM DCMU in photophobotaxis experiments	Figure 3H and Table 2
Biofilm in MV photophobotaxis experiments smaller than wild type	Figure 8F

of other species, the GAF domains of PixJ incorporate phycocyanobilin chromophores and undergo light-induced absorbance changes.[39] Like PixJ of *Anacystis nidulans*, PixJ of *P. lacuna* has four GAF domains (Figure 2D), three of which have a cysteine for chromophore attachment and can incorporate a bilin chromophore and undergo photoconversion. GAF domains bound to PCB chromophores absorb light between 400 and 760 nm.[40–42] The PixJ GAF domain of *Thermosynechococcus elongatus* and the second of the five PixJ GAF domains of *Synechococcus elongatus* absorb light in the green (530 nm) and blue ranges (430 nm),[10,43] but the full-length protein could absorb in diverse wavelengths regions.

PixJ also contains an MCP domain, which is known to be involved in chemotaxis in other systems.[44] Here, the MCP domain is part of the sensor of a chemical substance and modulates the sensitivity of this sensor toward the concentrations of the relevant chemical compound. Methylation and demethylation through CheR and CheB render the receptor less or more sensitive, respectively.[45] The signal is transmitted from the sensor to CheA histidine kinase. The role of PixJ as a negative photophobotaxis regulator can be utilized in this scheme. *P. lacuna* genome contains one *cheA*, two *cheR*, and one *cheB* genes. The *cheA* gene is located close to *pixJ* (Figure 2B). All proteins for adaptation by methylation and onset of signal transduction are thus present in *P. lacuna*. The questions of what triggers the adaptation and where PixJ stands in the context of photophobotaxis remain to be resolved.

Broad spectral activity points to photosynthesis pigments as sensor

PixJ and CphA, have an inhibitory or a weak positive effect on photophobotaxis, respectively. Neither of these must be regarded as photoreceptors for photophobotaxis, that is, a molecule that is responsible for light direction sensing. *P. lacuna* photophobotaxis was induced by a broad range of wavelengths, from 467 to 750 nm. The wild-type response to long-wavelength light (700 and 750 nm) was weak, but clear responses were obtained with the *pixJ* mutant (Figure 6). This broad spectral range indicates that different pigments are involved in light-direction sensing, because the spectral range of single photoreceptors is considerably narrower. *P. lacuna* has 28 cyanobacteriochromes and some of these could act together for the broad spectral activity of photophobotaxis. However, photosynthesis with its broad spectral absorbance seems a more likely candidate as photophobotaxis sensor. The DCMU effects and the sensitivity discussed below speak in favor of photosynthetic pigments.

The role of photosynthesis in light direction sensing

DCMU, a PS II electron flow inhibitor, inhibits photophobotaxis at 100 and 1000 μM concentrations. After 2 days of illumination at all DCMU concentrations, the wild-type filaments remained motile (Figures 8 and 9). Although motility was restricted in many cases, accumulation in the light cone would still be possible, if light sensing would work. Therefore, we concluded that DCMU could act specifically on light direction sensing and not in a general manner, for example, by cell death. This in turn could mean that photosynthesis pigments are used for sensing the light in photophobotaxis. The rather high concentration of DCMU required to achieve complete inhibition could indicate that only a small subfraction of PS II is required for light direction sensing.

MV also inhibited photophobotaxis but at higher concentrations than DCMU. The effect of MV concentration on photophobotaxis was comparable to that on motility. Therefore, we assume that MV inhibits photophobotaxis in a more general manner than DCMU by affecting filament vitality. Thus, light direction sensing is mediated through PS II rather than PS I. However, the photophobotaxis differences observed between the MV results of the three different strains suggest that PS I has some impact on photophobotaxis. For example, *pixJ* was more sensitive to inhibition by MV, which could be the result of photophobotaxis dysregulation. The impact of MV could occur via feedback from PS I on PS II.

In addition to the DCMU inhibition experiments and the broad spectral sensitivity of photophobotaxis, the sensitivity of the system to low-intensity light indicated that photosynthetic pigments could act as light direction sensors. In the eyes of animals, high rhodopsin pigment densities allow vision down to low light intensities.[46] The concentration of photosynthesis pigments in cyanobacteria is similarly high, whereas the concentration of standard photoreceptors such as phytochromes is

much lower. We calculated for a standard photoreceptor system, how many photoreceptors would be converted at a light sensitivity of 0.01 µmol $m^{-2} s^{-1}$, which induced a clear response in *pixJ*, and an irradiation time of 2 min. The parameters used for our calculation are cell dimensions of 4×4×4 $µm^3$,[21] a photoreceptor extinction coefficient of 100,000 $M^{-1} s^{-1}$, a photoconversion quantum yield of 0.15, and a photoreceptor concentration of 0.1 µM. This value was taken from phytochrome concentrations of etiolated maize seedlings[47] and *Agrobacterium fabrum*,[48] which both were reported to have phytochrome concentrations of 0.1 µM. With these parameters, we estimated the number of photoconverted photoreceptors per cell to 4. It is unlikely that such a low number can regulate the reversal of movement direction. The concentration of chlorophyll in *P. lacuna* as determined by UV–vis spectroscopy was 7 mM. Even if only a small fraction of chlorophyll were used for light direction sensing, many more molecules are converted by the light than the four molecules for a standard photoreceptor. Note that in plants very low fluence responses {Casal, 1998 #19816} are even more sensitive. The role of phytochrome in these responses is clear, but plant cells are much larger than *P. lacuna* cells and will have more photoreceptors per cell.

The specific inhibition of photophobotaxis by DCMU, broad spectral sensitivity, and the photophobotactic effect of very low light intensities all favor photosynthesis as a photoreceptor. We would like to mention that with our present knowledge a role of photoreceptor is not completely ruled out, and it is also possible that photoreceptors and photosynthesis act together in light direction sensing. The DCMU requires rather high concentrations which still could act in a non-specific manner. The sensitivity to low light can be explained by higher photoreceptor concentrations. The broad spectral activity could be explained by different photoreceptors.

Nevertheless, we aim to consider additional details, particularly if photosynthesis serves as the light sensor. Photosynthesis is based on light induced electron transfer driven by PS II and PS I. The first molecule along the photosynthetic electron transport path that leaves PS II is plastoquinone B (PQ_B). The PQ_ B-binding site is also a binding site for DCMU. Within PS II, PQ_B receives electrons from PQ_A, and the reduced form, PQ_B_H2, dissociates from PS II and delivers electrons to the cytochrome b6 f complex. A PQ_B_H2 sensor can then transmit the light signal to the next step in signal transduction (model in Figure 12). PQ_B is a transition from highly concentrated photosynthetic proteins to a low concentration signaling protein. Only a small fraction of the reduced PQ_B was expected to be utilized for sensing. Adaptation by PixJ could occur at this level, for example, by interference with the PQ_B sensor. We note that the adaptation of photosynthesis-based light sensing, mediated through a chromoprotein/photoreceptor, can change spectral sensitivity of this sensing. The fact that only a low fraction of activated PS II is enough for light direction sensing could elucidate why high DCMU concentrations are required for inhibiting photophobotaxis, whereas growth is inhibited at much lower concentrations.

General role of photosynthesis in light direction sensing of cyanobacteria

The high likelihood for photosynthesis in light-direction sensing raises the question whether photosynthesis can sense the direction of light in other cyanobacteria. We also performed photophobotaxis experiments using the

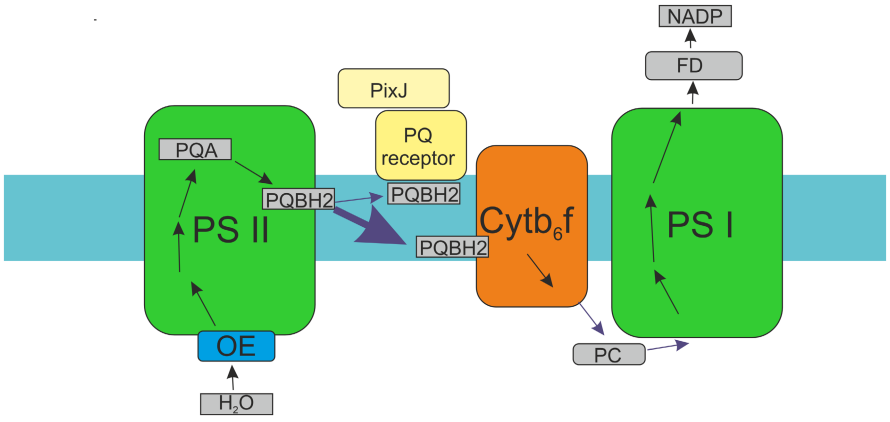

FIGURE 12 Cartoon of photosystem electron transport chain and proposed signal output. Black arrows indicate the flow of electrons, violet arrows indicate molecule flow. Gray boxes stand for small molecules, green boxes for PS I and PS II. PQBH2 stands for PQB in the reduced form.

single-celled cyanobacterium *Synechocystis* sp. PCC 6803. This species is probably the most used cyanobacterium in research, and most phototaxis experiments have been performed with it.[5,7,49,50] According to our expertise with *P. lacuna*, we performed photophobotaxis instead of phototaxis experiments. We found that *Synechocystis* sp. PCC 6803 also undergoes photophobotaxis and that this effect is inhibited by DCMU. Thus, photophobotaxis in this species could also be mediated by photosynthesis. Since the mechanisms of photophobotaxis and phototaxis differ, both are not necessarily mediated by the same light sensors. Wilde[5] reported a DCMU effect on phototaxis under blue light, but no effect under red or white light; in another work, Choi et al.[20] found no DCMU effect on phototaxis. However, it is also possible that these authors used concentrations that were not sufficiently high; in our experiments, the inhibitory concentration was quite high. All in all could the role of photosynthesis as light direction sensor in light direction sensing of cyanobacteria play a more prominent role that was overseen for several reasons.

PixJ was the linking element between species and responses. This protein affects phototaxis or photophobotaxis in all evaluated cyanobacterial species. If PixJ modulates light direction sensing in *P. lacuna*, this could also be true for other cyanobacteria. Although in our system, PixJ is not the photoreceptor itself for light direction sensing, the clue for the molecular mechanisms of PixJ will clarify the light direction sensing by photosynthesis.

ACKNOWLEDGMENTS

We thank Henrik Früh (master's student of biology, KIT) for help with the infrared time-lapse camera system. We acknowledge the help of Gernot Guigas (Physics Department, KIT) with differential equations, Daniel Gotman for technical help in several respects, and Anna-Lena Klemke for help with the *pixJ* knockout vector cloning. Open Access funding enabled and organized by Projekt DEAL.

ORCID

Tilman Lamparter https://orcid.org/0000-0003-4327-9737

REFERENCES

1. Lazar T. Taiz, L. and Zeiger, E. Plant physiology. 3rd edn. *Ann Bot*. 2003;91:750-751.
2. Kamennaya NA, Ajo-Franklin CM, Northen T, Jansson C. Cyanobacteria as biocatalysts for carbonate mineralization. *Minerals*. 2012;2:338-364.
3. Halldal P. Importance of calcium and magnesium ions in phototaxis of motile green algae. *Nature*. 1957;179:215-216.
4. Narikawa R, Suzuki F, Yoshihara S, Higashi S, Watanabe M, Ikeuchi M. Novel photosensory two-component system (PixA-NixB-NixC) involved in the regulation of positive and negative phototaxis of cyanobacterium *Synechocystis* sp PCC 6803. *Plant Cell Physiol*. 2011;52:2214-2224.
5. Wilde A, Fiedler B, Borner T. The cyanobacterial phytochrome Cph2 inhibits phototaxis towards blue light. *Mol Microbiol*. 2002;44:981-988.
6. Haeder DP, Nultsch W. Negative photo-phobotactic reactions in *Phormidium-uncinatum*. *Photochem Photobiol*. 1973;18:311-317.
7. Bhaya D, Takahashi A, Grossman AR. Light regulation of type IV pilus-dependent motility by chemosensor-like elements in *Synechocystis* PCC6803. *Proc Natl Acad Sci USA*. 2001;98:7540-7545.
8. Lamparter T, Babian J, Frohlich K, et al. The involvement of type IV pili and the phytochrome CphA in gliding motility, lateral motility and photophobotaxis of the cyanobacterium *Phormidium lacuna*. *PLoS One*. 2022;17:e0249509.
9. Schuergers N, Lenn T, Kampmann R, et al. Cyanobacteria use micro-optics to sense light direction. *Elife*. 2016;5:e12620.
10. Yang Y, Lam V, Adomako M, et al. Phototaxis in a wild isolate of the cyanobacterium *Synechococcus elongatus*. *Proc Natl Acad Sci USA*. 2018;115:E12378-E12387.
11. Conradi FD, Mullineaux CW, Wilde A. The role of the cyanobacterial type IV pilus machinery in finding and maintaining a favourable environment. *Life*. 2020;10:252.
12. Yoshihara S, Ikeuchi M. Phototactic motility in the unicellular cyanobacterium *Synechocystis* sp. PCC 6803. *Photochem Photobiol Sci*. 2004;3:512-518.
13. Fiedler B, Borner T, Wilde A. Phototaxis in the cyanobacterium *Synechocystis* sp. PCC 6803: role of different photoreceptors. *Photochem Photobiol*. 2005;81:1481-1488.
14. Sugimoto Y, Masuda S. In vivo localization and oligomerization of PixD and PixE for controlling phototaxis in the cyanobacterium *Synechocystis* sp. PCC 6803. *J Gen Appl Microbiol*. 2021;67:54-58.
15. Sugimoto Y, Nakamura H, Ren S, Hori K, Masuda S. Genetics of the blue light-dependent signal cascade that controls phototaxis in the cyanobacterium *Synechocystis* sp PCC6803. *Plant Cell Physiol*. 2017;58:458-465.
16. Song JY, Cho HS, Cho JI, Jeon JS, Lagarias JC, Park YI. Near-UV cyanobacteriochrome signaling system elicits negative phototaxis in the cyanobacterium *Synechocystis* sp PCC 6803. *Proc Natl Acad Sci USA*. 2011;108:10780-10785.
17. Ud-Din A, Roujeinikova A. Methyl-accepting chemotaxis proteins: a core sensing element in prokaryotes and archaea. *Cell Mol Life Sci*. 2017;74:3293-3303.
18. Hader DP. Participation of 2 photosystems in photo-phobotaxis of *Phormidium-uncinatum*. *Arch Microbiol*. 1974;96:255-266.
19. Harwood TV, Zuniga EG, Kweon H, Risser DD. The cyanobacterial taxis protein HmpF regulates type IV pilus activity in response to light. *Proc Natl Acad Sci USA*. 2021;118:e2023988118.
20. Choi JS, Chung YH, Moon YJ, et al. Photomovement of the gliding cyanobacterium *Synechocystis* sp. PCC 6803. *Photochem Photobiol*. 1999;70:95-102.
21. Nies F, Worner S, Wunsch N, et al. Characterization of *Phormidium lacuna* strains from the North Sea and the Mediterranean Sea for biotechnological applications. *Process Biochem*. 2017;59:194-206.

22. Guillard RR, Ryther JH. Studies of marine planktonic diatoms. I. Cyclotella nana Hustedt, and *Detonula confervacea* (cleve) Gran. *Can J Microbiol*. 1962;8:229-239.
23. Nies F, Mielke M, Pochert J, Lamparter T. Natural transformation of the filamentous cyanobacterium *Phormidium lacuna*. *PloS One*. 2020;15:e0234440.
24. Weber N, Hofmeister M, Wunsch N, et al. Natural transformation, protein expression, and cryoconservation of the filamentous cyanobacterium *Phormidium lacuna*. *J Vis Exp*. 2022:e63470.
25. Mann HB, Whitney DR. On a test of whether one of 2 random variables is stochastically larger than the other. *Ann Math Stat*. 1947;18:50-60.
26. Xiong J, Subramaniam S, Govindjee. Modeling of the D1/D2 proteins and cofactors of the photosystem II reaction center: implications for herbicide and bicarbonate binding. *Protein Sci*. 1996;5:2054-2073.
27. Petrova IV, Myasnik MN, Skvortsov VG. The combined effect of photoreactivation and temperature on the survival of E. Coli B cells exposed to far UV-light. *Radiobiologiia*. 1984;24:595-598.
28. Yeh KC, Wu SH, Murphy JT, Lagarias JC. A cyanobacterial phytochrome two-component light sensory system. *Science*. 1997;277:1505-1508.
29. Paul R, Weiser S, Amiot NC, et al. Cell cycle-dependent dynamic localization of a bacterial response regulator with a novel diguanylate cyclase output domain. *Genes Dev*. 2004;18:715-727.
30. Moon YJ, Kim SY, Jung KH, Choi JS, Park YM, Chung YH. Cyanobacterial phytochrome Cph2 is a negative regulator in phototaxis toward UV-A. *FEBS Lett*. 2011;585:335-340.
31. Narikawa R, Ishizuka T, Muraki N, Shiba T, Kurisu G, Ikeuchi M. Structures of cyanobacteriochromes from phototaxis regulators AnPixJ and TePixJ reveal general and specific photoconversion mechanism. *Proc Natl Acad Sci USA*. 2013;110:918-923.
32. Finn RD, Bateman A, Clements J, et al. Pfam: the protein families database. *Nucleic Acids Res*. 2014;42:D222-D230.
33. Narikawa R, Fushimi K, Ni Ni W, Ikeuchi M. Red-shifted red/green-type cyanobacteriochrome AM1_1870g3 from the chlorophyll d-bearing cyanobacterium *Acaryochloris marina*. *Biochem Biophys Res Commun*. 2015;461:390-395.
34. Koenig F. Shade adaptation in cyanobacteria - further characterization of *Anacystis* shade phenotype AS induced by sublethal concentrations of DCMU-type inhibitors in strong light. *Photosynth Res*. 1990;26:29-37.
35. Summers LA. *The Bipyridinium Herbicides*. Academic Press; 1980.
36. Knobloch JK, Bartscht K, Sabottke A, Rohde H, Feucht HH, Mack D. Biofilm formation by Staphylococcus epidermidis depends on functional RsbU, an activator of the sigB operon: differential activation mechanisms due to ethanol and salt stress. *J Bacteriol*. 2001;183:2624-2633.
37. Simm R, Morr M, Kader A, Nimtz M, Römling U. GGDEF and EAL domains inversely regulate cyclic di-GMP levels and transition from sessility to motility. *Mol Microbiol*. 2004;53:1123-1134.
38. Angerer V, Schwenk P, Wallner T, Kaever V, Hiltbrunner A, Wilde A. The protein Slr1143 is an active diguanylate cyclase in *Synechocystis* sp PCC 6803 and interacts with the photoreceptor Cph2. *Microbiology*. 2017;163:920-930.
39. Tarutina M, Ryjenkov DA, Gomelsky M. An unorthodox bacteriophytochrome from *Rhodobacter sphaeroides* involved in turnover of the second messenger c-di-GMP. *J Biol Chem*. 2006;281:34751-34758.
40. Fushimi K, Narikawa R. Phytochromes and cyanobacteriochromes: photoreceptor molecules incorporating a linear tetrapyrrole chromophore. *Adv Exp Med Biol*. 2021;1293:167-187.
41. Xu QZ, Bielytskyi P, Otis J, et al. MAS NMR on a red/far-red photochromic cyanobacteriochrome All2699 from *Nostoc*. *Int J Mol Sci*. 2019;20:3656.
42. Moreno MV, Rockwell NC, Mora M, Fisher AJ, Lagarias JC. A far-red cyanobacteriochrome lineage specific for verdins. *Proc Natl Acad Sci USA*. 2020;117:27962-27970.
43. Burgie ES, Clinger JA, Miller MD, et al. Photoreversible interconversion of a phytochrome photosensory module in the crystalline state. *Proc Natl Acad Sci USA*. 2020;117:300-307.
44. Gegner JA, Graham DR, Roth AF, Dahlquist FW. Assembly of an MCP receptor, CheW, and kinase CheA complex in the bacterial chemotaxis signal transduction pathway. *Cell*. 1992;70:975-982.
45. Karmakar R. State of the art of bacterial chemotaxis. *J Basic Microbiol*. 2021;61:366-379.
46. Detwiler PB, GrayKeller MP. The mechanisms of vertebrate light adaptation: speeded recovery versus slowed activation. *Curr Opin Neurobiol*. 1996;6:440-444.
47. Butler WL, Lane HC, Siegelman HW. Nonphotochemical transformations of phytochrome *in vivo*. *Plant Physiol*. 1963;38:514-519.
48. Oberpichler I, Molina I, Neubauer O, Lamparter T. Phytochromes from *Agrobacterium tumefaciens*: difference spectroscopy with extracts of wild type and knockout mutants. *FEBS Lett*. 2006;580:437-442.
49. Nam M-H, Choi J-S, Chung Y-H, Kim S-H, Woo J-C, Park Y-M. Effects of some metabolic inhibitors on phototactic movement in cyanobacterium *Synechocystis* sp. PCC 6803. *J Plant Biol*. 1995;38:87-93.
50. Wilde A, Mullineaux CW. Light-controlled motility in prokaryotes and the problem of directional light perception. *FEMS Microbiol Rev*. 2017;41:900-922.

SUPPORTING INFORMATION

Additional supporting information can be found online in the Supporting Information section at the end of this article.

How to cite this article: Schwabenland E, Jelen CJ, Weber N, Lamparter T. Photophobotaxis in the filamentous cyanobacterium *Phormidium lacuna*: Mechanisms and implications for photosynthesis-based light direction sensing. *Photochem Photobiol*. 2024;100:1290-1309. doi:10.1111/php.13908